Reports

Sherman Landslide, Alaska

Abstract. *Triggered by the earthquake of 27 March 1964, 3 × 10^7 cubic meters of rock fell 600 meters, then slid at high speed 5 kilometers across the nearly level Sherman glacier near Cordova. The landslide has a number of significant new features in addition to those typical of other large landslides that may have slid on a layer of trapped and compressed air.*

One of the largest of the many avalanches triggered by the Alaska earthquake of 27 March 1964 was the Sherman landslide in the rugged Chugach Mountains 25 km east of Cordova, Alaska, and 130 km east of the epicenter of the earthquake (*1*). A steeply dipping, pervasively jointed, tabular block of massive sandstone and argillite roughly 450 m long, 300 m wide, and 150 m thick that comprised the west face and uppermost 50 m of a Matterhorn-like peak, now informally called "Shattered Peak" (60°32′N, 145°06′W), was shaken free along a bedding surface and plunged 600 m down the 40-degree slope below, then slid as far as 5 km northwestward across the gently sloping, snow-covered terminal reach of the Sherman Glacier (Figs. 1 and 2). The mass (3 × 10^7 m^3) of debris spread out in a crudely trapezoidal, partially digitate lobe having an average width of about 1.5 km, a maximum width of nearly 3 km, and a relatively uniform thickness of 3 to 6 m. It evidently traveled at high speed, for it surmounted a spur ridge rising 140 m athwart its southern edge, and it climbed 25 m up the opposite valley wall at its northern edge.

The Sherman landslide has attracted attention not only because of its large size and spectacular origin but also because it covers a considerable fraction of the lower end of the glacier with a highly insulating blanket of debris, which by July 1965 had already prevented the normal loss of several meters of ice. Investigators from a number of organizations are studying the expected advance of the terminus and its effect upon the proglacial and superglacial plant and animal communities (*2*).

The landslide is noteworthy also because it possesses the peculiar association of features characteristic of several other large landslides, best typified by the Blackhawk (Tables 1 and 2), which I have proposed slid on a cushion of compressed air trapped in the initial fall (*6*). The Sherman, however, has in addition a number of new features not reported in the other Blackhawk-type landslides; and it differs from them in its relatively large content of snow and strongly divergent pattern of movement.

The landslide debris consists almost entirely of sharply angular and sur-

Fig. 1. Sherman landslide, Alaska, viewed from west. Debris fell from high peak at right during Alaska earthquake of 27 March 1964. It slid at high speed across the 2.5-km width of the Sherman Glacier, surmounting the 140-m spur ridge at right and climbing 25 m up valley wall at left, Thickness of debris is 3 to 6 m; volume is 3 × 10^7 m^3. Glacier is expected to advance as result of insulating effect of debris. Photograph by Austin Post, U.S. Geological Survey, 25 August 1965 (F654 189).

Table 1. Data on Blackhawk-type landslides.

Landslide	Type of source	Debris		"Coefficient of friction"*	Height climbed (m)	Minimum speed† (km hr^{-1})
		Principal lithology	Volume (m^3)			
Elm (*3*) (11 Sept. 1881)	Undermined cliff	Slate	1×10^7	0.26	100	160
Sherman (27 Mar. 1964)	Undercut dipslope	Sandstone	3×10^7	.22	140 25	185 80
Frank (*4*) (29 Apr. 1903)	Undercut thrust block	Limestone	4×10^7	.26	120	175
Silver Reef (*6*) (Prehistoric)	Undercut thrust block	Limestone	23×10^7	.13	45	105
Blackhawk (*6*) (Prehistoric)	Undercut thrust block	Limestone	28×10^7	.13	60	120
Saidmarreh (*5*) (Prehistoric)	Undercut dipslope	Limestone	420×10^7	.10	450	330

* Maximum drop divided by overall length. † Computed on the assumption of simple conservation of energy.

prisingly unbruised fragments of sandstone. Other constituents, much less abundant, are crushed argillite, dirty snow, and traces of wood, sod, moss, grass, and morainal granite gneiss. Throughout the landslide lobe, but especially toward its eastern margin, only a small fraction of the external surfaces of the fragments is freshly broken, completely unweathered rock; hence, the source block evidently was pervasively jointed and fractured long before it fell. On the landslide surface the debris is generally the size of boulders; these are loosely piled and highly unstable. Scattered exposures in crevasse walls indicate that beneath the surface, however, the material is finer grained, tightly packed, and relatively nonporous. Where it is exposed the base of the debris is in sharp contact with either foliated glacier ice or undisturbed stratified snow.

The sandstone is a gray, hard, massive, unbedded, coarse-grained graywacke that turns yellow to brown with weathering. Locally it contains numerous interlaced veinlets and nodules of milky quartz. The sandstone fragments in the landslide debris range in size from powder to boulders 10 to 20 m long, the modal diameter at the surface being approximately 25 to 50 cm. The biggest fragment in the landslide is a truncated pyramidal monolith of sandstone measuring 15 by 20 m at the base and more than 17 m high (Fig. 3). One face of this block, approximately 12 by 12 m in extent, has lichens, moss, and even soil and clumps of grass clinging to it, indicating that it is part of the original weathered face of the mountain. Similarly lichen-covered and, in many cases, also glacially striated surfaces are present on most of the other unusually large blocks, all of them sandstone, scattered along the eastern margin of the landslide.

This diffuse segregation of fragments having certain characteristics in common, such as striated surfaces, deeper weathering, or greater size, is present throughout the landslide, except close to the edges and to the lee of the spur ridge. At one extreme in scale is the three-dimensional jigsaw puzzle effect, observed at a number of localities, in which individual large blocks are shat-

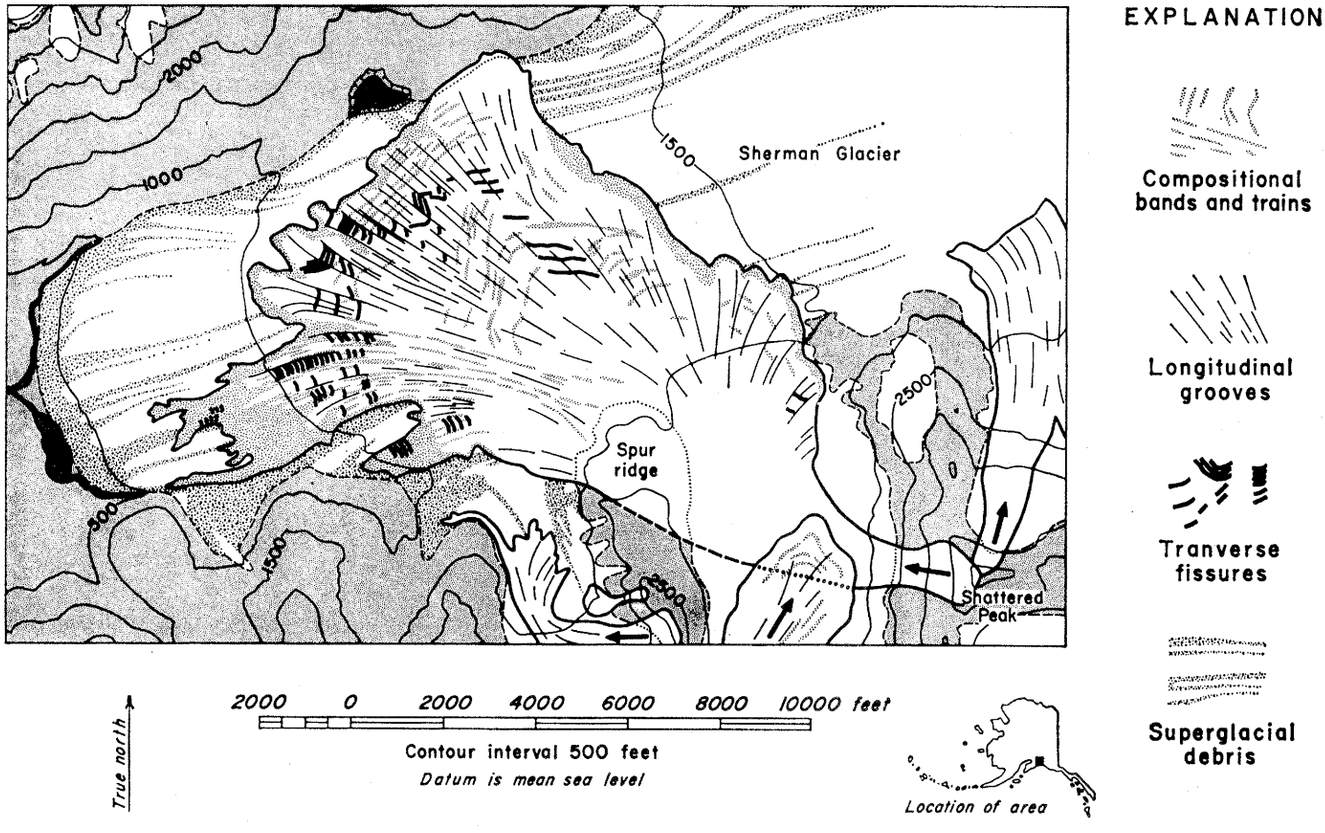

Fig. 2. Sketch map of Sherman landslide showing schematically compositional bands, compositional trains, longitudinal grooves, and transverse fissures. Topographic base map after U.S. Geological Survey Cordova C-3 and C-4 quadrangles, Alaska (scale 1:63360).

tered yet undisaggregated. At the other extreme are the diffuse, subparallel, roughly transverse textural and compositional bands shown in aerial photographs and confirmed by ground observations (Fig. 2). A similar tendency toward local homogeneity in the debris is also typical of the other landslides of the Blackhawk type (Table 2). This tendency implies an absence of large-scale mixing in the motion of the avalanche, inasmuch as the common characteristics can only arise from common provenance.

The argillite is black, hard, nonfissile, and turns rust-colored with weathering. In places it is interbedded with irregular thin sandy layers. It is more easily crushed than the sandstone; individual fragments range in size from powder to boulders 2 to 3 meters long, the modal diameter at the surface being about 2 to 3 cm. It is present throughout the landslide in isolated blocks, clusters of blocks, and scattered diffuse bands of fragments; but it is quantitatively significant only in the relatively heterogeneous debris near the distal and lateral edges of the landslide lobe and in the lee of the overtopped spur ridge.

In the latter locality the debris is arranged in distinctive diffuse compositional trains, mostly 30 to 60 m wide, whose axes parallel the local direction of movement (Fig. 2). Trains of coarser debris containing little argillite alternate with trains of finer debris which is rich in argillite; the coarser trains appear to originate at high points on the lee slope of the spur ridge.

On the spur ridge itself the debris consists almost entirely of sandstone boulders ranging up to 4 to 5 m in length, the modal diameter being about 20 to 40 cm. As elsewhere, the material beneath the surface appears to be finer and solidly packed. The debris mantles stoss slopes and hill tops to a depth of 2 or 3 m, but on lee slopes alders, moss, and small plants are completely undisturbed, a fact which further confirms the high speed of the landslide.

The snow within the debris, in contradistinction to that beneath it, is unstratified and, although it appears clean in fresh exposures, it contains a uniformly distributed sparse admixture of sand and fine gravel which accumulates as a lag concentrate on weathered surfaces. It is most abundant at the distal edges of the landslide, where it commonly comprises almost the full thickness of the debris and undoubtedly corresponds to the wedge of bulldozed and transported rubble embedded in the distal edges of the other large landslides of the Blackhawk type (Table 2). Elsewhere the snow appears to form a discontinuous basal layer up to 1 or 2 m thick. The top of this basal layer merges with the overlying layer of snow-free rock debris in a gradational contact a few centimeters thick. In scattered localities, particularly over the larger glacier crevasses near the northern and eastern edges of the landslide, this underlying snow has erupted through fissures in the denser overlying rock debris. When these snow upwellings melt, they characteristically deposit a sharply delimited patch of finer-grained, less homogeneous debris on the surface surrounding the fissure.

Table 2. Features of Blackhawk-type landslides.

Landslide	Air launch	Local homogeneity of debris	Wedge of transported debris	Lateral ridges	Distal rim	Transverse surface pattern	Jigsaw puzzle effect	Debris cones
Elm	Observed	Yes	Yes	2	Yes	Yes	?	Yes
Sherman	Probable	Yes	Yes	Many	Yes	Local*	Yes	Yes
Frank	Observed	Yes	Yes	1	Yes	Yes	?	Yes
Silver Reef	Possible	Yes	Yes	2	Yes	Yes	Yes	?
Blackhawk	Probable	Yes	Yes	2	Yes	Yes	Yes	?

* In debris buttresses and distal rim; dominant pattern is longitudinal grooves cut by transverse fissures.

The wood in the landslide is mostly broken and splintered alder from the overtopped spur ridge. It is present only at the distal edge of the landslide lobe, indicating that, as in the other landslides of the Blackhawk type the debris did not flow like a viscous fluid but instead slid like a flexible sheet. This conclusion is further supported by the fact that the underlying topography of the glacier is plainly reflected in the landslide surface. Thus, the low "coefficient of friction" is due, not to low internal friction, but to low sliding friction.

The edges of the landslide lobe are bounded by the lateral ridges and distal rim typical of landslides of the Blackhawk type (Table 2). They are 3 to 15 m high, 15 to 150 m wide, chaotically hummocky in topography (Fig. 4), and in places imbricate in structure. The lateral edges have the same distinctive heterogeneous lithology rich in argillite as the distal rim, a fact which implies that they were deposited at the flanks of the leading edge of the sliding debris.

The western half of the landslide split into multiple minor lobes, each with low lateral ridges and a prominent distal rim. The points of separation are invariably occupied by wedge-like raised buttresses of debris rich in argillite (Fig. 4). These buttresses evidently are narrow sections of distal rim that prematurely came to rest.

The most striking feature of the Sherman landslide is the pattern of parallel shallow V-shaped longitudinal grooves that cover the entire surface of the landslide lobe except the lateral ridges and distal rim (Figs. 2 and 4). They vary in size up to 8 m wide, 600 m long, and a couple of meters deep. Individual grooves usually broaden slightly in the distal direction; and at their ends they normally merge imperceptibly with the landslide surface, although they occasionally terminate abruptly at large blocks. In general, however, they appear to be distributed independently of the large blocks. Pronounced differences in lithology between the two walls of several of the more prominent grooves indicate that they were formed by shear between substreams of debris advancing at different speeds or times. The grooves within these substreams, which comprise the vast majority, do not appreciably offset the transverse compositional bands, however, and hence could not have been formed by shear. Therefore, although they are parallel to the direction of sliding, they cannot be analogous to flow bands in rocks. Perhaps they are simply multiple narrow splits caused by the divergent motion of the debris and partially filled by debris slumping from the sides.

Similar longitudinal grooves are present on a number of smaller contemporaneous landslides in the vicinity of the Sherman, but they are not mentioned in the descriptions of the other large landslides of the Blackhawk type. An obvious difference is the presence of the discontinuous basal layer of snow, which may have provided the cohesion needed to cause pervasive splitting rather than uniform spreading.

The landslide lobe interior to the lateral ridges and distal rim is cut by

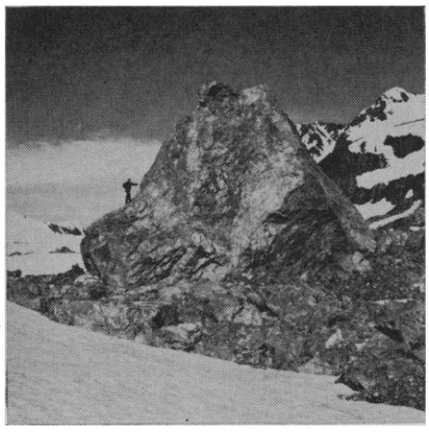

Fig. 3. Largest boulder in landslide. It measures 15 by 20 m at the base and more than 17 m in height. Righthand face still has lichens, moss, and even soil and clumps of grass clinging to it. Photograph by the author, 9 July 1965.

numerous transverse tension fissures (Fig. 4), which are unrelated to the underlying glacier crevasses. Except in the distal rim, therefore, the Sherman landslide was not subject to the compression and imbrication typical of other landslides of the Blackhawk type (Table 2). Thus, the presence of the longitudinal grooves on the Sherman could also be due to the preservation of splits that were destroyed by the piling up of debris in the other landslides.

The transverse fissures appear as swarms of parallel, irregularly sinuous, deep V-shaped or flat-bottomed trenches (Fig. 2) 3 to 15 m wide, 1 to 5 m deep, up to 150 m long, and separated from each other by distances usually two to three times their width. With few exceptions they end at lateral ridges or at grooves bounding subparallel streams in the debris. In plan most are concave toward the distal edge, their ends oriented about 45 degrees to the direction of sliding, indicating that drag from beneath was negligible compared with that from the sides. This finding further supports the conclusion that the debris slid rather than flowed.

Perhaps the most interesting and certainly the most puzzling of the minor features of the Sherman landslide are the cones of tightly packed finer-grained debris, like that beneath the landslide surface, which are piled at the angle of repose atop certain boulders. At least several hundred of these debris cones are scattered over the entire surface of the landslide, with the greatest density being toward the centerline and about 150 to 300 m from the distal edge. A few are isolated but most are clustered in groups. None are located in longitudinal grooves or transverse fissures. Boulders with cones are usually larger than the local average, attaining a maximum diameter of about 5 m. Like many roughly equant cone-free large boulders on the landslide, they commonly sit in close-fitting steep-walled shallow pits in the debris. Boulders are invariably present under the cones, although sometimes they are hidden by sloughed-off rubble. On the other hand, even in the most densely populated clusters not all of the apparently eligible boulders have cones.

Perhaps two thirds of the cones, like those reported from other landslides of the Blackhawk type (Table 2), are not lithologically distinguishable from the surrounding debris, whereas the remainder are, some of them strikingly so. At least 25 of these xenolithologic debris cones and their underlying boulders, for example, consist entirely of argillite, whereas the surrounding debris consists entirely of sandstone (Fig. 5). More commonly, however, the contrast is between different varieties of the sandstone. In many instances both cone and boulder have identical peculiarities of lithology; and in one case a group of seven xenolithologic cones as much as 60 m apart not only consist of the same distinctive red-weathered sandy argillite but also stand upon the separated but unrotated fragments of a single large boulder of the same material.

Fig. 5. Xenolithologic debris cone. Cone and underlying boulder are argillite; surrounding debris is sandstone. Length of ice axe is about 90 cm. Photograph by the author, 9 July 1965.

According to the hypothesis of air-layer lubrication, huge rockfalls like the Sherman and the other landslides of the Blackhawk type acquire so much momentum in their initial fall that at a break in slope they leave the ground, overriding and trapping a cushion of compressed air upon which they slide at high speed with little friction (*6*). The Sherman undoubtedly was launched into the air at the top of the glacially oversteepened foot of Shattered Peak; but direct evidence is lacking that it trapped sufficient air long enough to account for the low friction implied by the sustained speed and long runout, by the distribution of wood fragments and bulldozed snow, by the local homogeneity and compositional bands in the debris, and by the pattern of the transverse fissures. Water and mud as lubricants, strong possibilities in the other landslides of the Blackhawk type, are ruled out by the subfreezing temperature at the time of the landslide, leaving only dry snow or perhaps a slurry of snow and air as likely alternatives (*7*). Both possibilities certainly must have been in-

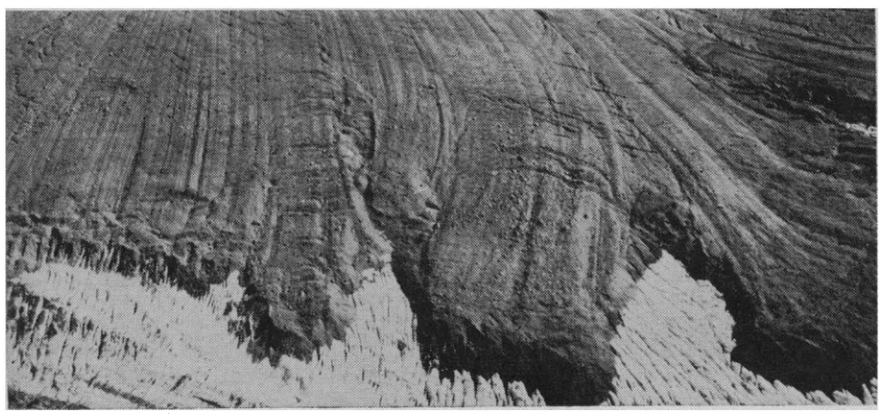

Fig. 4. Surface and distal edge of landslide. Viewed from north. Motion of landslide toward observer. Width of lobe in center foreground about 300 m. Note raised distal rim, debris buttresses at vertices between lobes, longitudinal grooves, and transverse fissures on surface. Photograph by Austin Post, U.S. Geological Survey, 25 August 1965 (F654 184).

volved, and they may even have been important in the formation of the parallel longitudinal grooves on the landslide surface and the narrow flow-like lobes at its western edge. Air as the primary lubricant, however, accounts more simply for the pronounced terminal increase in friction suggested by some of the other features of the landslide. Leakage of air from beneath the flanks of the leading edge, for example, being unopposed by the forward motion of the landslide, would very quickly permit the margin to settle to the glacier surface and stop, forming the lateral ridges, which would channel the sliding debris and hinder further leakage. Similarly, the slower but inevitable loss of air at the leading edge would ultimately allow it to hit the surface, causing the debris behind to pile up. Initially this would occur at overwidened longitudinal grooves, forming the debris buttresses, which would split the sliding mass into multiple minor lobes; but eventually it would occur over the whole leading edge, forming the distal rim. Finally, the progressive thinning of the air layer at the rear of the landslide, as ever more air is dragged forward by the sliding debris, would cause widespread zones of impact to form and propagate forward, producing the swarms of successive transverse tension fissures. Thus, although direct evidence is lacking, the circumstantial evidence strongly supports the hypothesis of air-layer lubrication for the Sherman landslide.

RONALD L. SHREVE
Department of Geology and *Institute of Geophysics and Planetary Physics, University of California, Los Angeles*

References and Notes

1. G. Plafker, *Science* **148**, 1675 (1965); R. H. Ragle, J. E. Sater, W. O. Field, *Arctic Institute of North America Res. Paper 32*; W. O. Field, *International Association of Scientific Hydrology Pub.* **69**, 326 (1965).
2. W. O. Field, *ibid.*; C. Marangunic and C. Bull, *Am. Geophys. Union Trans.* **47**, 81 (1966); L. Clayton, W. O Field, S. J. Tuthill, *ibid.*; S. J. Tuthill, *ibid.*, p. 82.
3. E. Buss and A. Heim, *Der Bergsturz von Elm den 11. September 1881* (Wurster, Zurich, 1881), p. 127; A. Heim, *Z. Deut. Geol. Ges.* **34**, 74 (1882); A. Heim, *Geologie der Schweiz* (Tauchnitz, Leipzig, 1921), vol. 2, pt. 1, p. 402; A. Heim, *Bergsturz und Menschenleben* (Fretz and Wasmuth, Zurich, 1932).
4. R. G. McConnell and R. W. Brock, *Canada Dept. Interior, Annual Rept. 1902-1903*, pt. 8, Rept. Supt. Mines, appendix (1904); R. A. Daly, W. G. Miller, G. S. Rice, *Canada Geol. Surv. Mem. 27* (1912).
5. J. V. Harrison and N. L. Falcon, *J. Geol.* **46**, 296 (1938).
6. R. L. Shreve, in preparation.
7. A number of people have suggested to me that the low friction is due simply to the high speed, an idea proposed in 1882 by A. Heim, *ibid.*, but this seems to me merely to describe the phenomenon without explaining it.
8. Supported by the American Geographical Society. I thank W. O. Field, American Geographical Society, for the necessary administrative arrangements and for photographs and other information; S. J. Tuthill, Muskingum College, Ohio, for use of base camp and helicopter (National Science Foundation grant GP 4424); and G. Plafker and A. Post, U.S. Geological Survey, for aerial photographs, topographic map, and general information. Publication No. 534, Institute of Geophysics and Planetary Physics, University of California, Los Angeles 90024.

20 September 1966

Calcium in Sea Water by Electrode Measurement

Abstract. *Ionized calcium in standard International Association of Physical Oceanography sea water (chlorinity, 19.373 parts per thousand) was measured with a recently developed, highly selective, calcium electrode. We found that 84 percent of the calcium in sea water exists as Ca++, in fair agreement with the 91 percent calculated for the chemical model of sea water of Garrels and Thompson. If one used the activity coefficient for calcium ion of Garrels and Thompson, 0.28, calcium-ion activity in this sea water would be 0.00249. Another activity coefficient for calcium ion in sea water, 0.24, derived from Berner's measured total-activity coefficient and our measurement of the fraction of ionized calcium, yields a slightly lower activity, 0.00214.*

A recently developed calcium electrode (*1*) was used to measure the percentage of ionized calcium in standard International Association of Physical Oceanography sea water of 19.373-ppt chlorinity. The electrode-potential measurements were made against a saturated KCl–calomel reference electrode by use of an expanded-scale voltmeter and a strip-chart recorder. Temperature was controlled at 25°±0.1°C, and the solutions were stirred magnetically.

The electrode is highly selective for calcium ion, and, if it is calibrated in solutions similar to the unknown, the effects of other cations or of moderate variations in *p*H may be neglected. The response to calcium is linear in the presence of a constant amount of other cations; that is, a plot of electrode potentials versus the log of calcium-ion activity is rectilinear over a range of calcium-ion concentration bracketing that of sea water. Of course, for preparations of such plots, assumptions must be introduced about single-ion activity coefficients. In the preliminary studies of the electrode behavior, the responses to calcium were measured in various aqueous solutions: NaCl, $MgCl_2$, NaCl + $MgCl_2$, and finally NaCl + $MgCl_2$ + KCl—each in its approximate sea-water concentration. The slope of the electrode response to calcium in solutions containing $MgCl_2$ was consistently steeper than would be predicted by a Nernst electrode equation such as:

$$E = E^0_{Ca} + 2.303(RT/2F) \log (Ca^{++})$$

in which E is the observed potential, E^0_{Ca} is an empirical constant. R, T, and F are as usually defined and (Ca^{++}) indicates a calculated calcium-ion activity. Moreover, unpredictable variations in the E^0_{Ca} term were observed, it being about 10 mv more positive in the NaCl than in the $MgCl_2$ solutions, and intermediate in the NaCl + $MgCl_2$ or the NaCl + $MgCl_2$ + KCl solutions. Because the slope measurements were made in solutions having nearly the same ionic strength, we could not rectify the data by changing the assumed single-ion activity coefficients. We finally concluded that changes in liquid-junction potential might explain the changes in E^0_{Ca}, and that it would be best to proceed empirically by calibrating the electrode in solutions having nearly the same ionic strength and sodium-, magnesium-, and potassium-ion content as the standard sea water.

With respect to anions, however, the problem is different. Sulfate, carbonate, and bicarbonate ions in sea water complex part of the cations, but there is no known complexing of these cations by chloride ions (*2*). In order to avoid introduction of any assumptions about magnitude of the effects of those anions on calcium ion, we made our calibrating solutions with

Table 1. Composition of calibrating solutions and of sea water of 19.373-ppt chlorinity, and electrode-potential measurements of the solutions.

Solution	Ion (M)				E (mv)		
	Na	K	Mg	Ca	1	2	3
No. 1	0.459	0.0097	0.0496	0.00516	−55.0	−55.0	−55.5
No. 2	.459	.0097	.0496	.01032	−43.9	−44.0	−44.3
Sea water	.469	.0097	.0534	.0102	−47.2	−47.0	−47.0